Tricritical and Critical End-Point Phenomena under Random Bonds

Alexis Falicov and A. Nihat Berker
Department of Physics, Massachusetts Institute of Technology, Cambridge, Massachusetts 02139
(Received 30 December 1994)

The effect of bond randomness on tricritical and critical end-point phenomena is studied by renormalization-group theory. In three dimensions, the pure-system tricritical point is replaced by a line segment of second-order transitions dominated by randomness and bounded by a multicritical point and a random-bond tricritical point, which reaches zero temperature at threshold randomness. This topology indicates a violation of the empirical universality principle. The random-bond tricritical point renormalizes onto the fixed distribution of random-field Ising criticality. [S0031-9007(96)00332-8]

PACS numbers: 64.60.Kw, 05.70.Jk, 75.10.Nr, 75.40.Cx

Although originally thought to play a rather innocuous role, quenched bond randomness can drastically affect first-order phase transitions. Thus, symmetry-breaking first-order phase transitions are converted to second-order phase transitions by infinitesimal bond randomness for spatial dimensionality $d \leq 2$ and by bond randomness beyond a threshold strength for $d > 2$, as indicated by general arguments [1–3] which are supported, for $d \leq 2$, by rigorous mathematical work [4] and renormalization-group calculations [5]. We present here renormalization-group calculations for $d = 3$, on the effects of quenched bond randomness on a system that exhibits first-order phase transitions within tricritical and critical end-point phase diagrams. We find that new second-order phase transitions are introduced, in violation of the empirical universality principle which states that, along the second-order phase boundary between any given two phases, critical exponents should not change. Furthermore, the effect of quenched bond randomness on tricritical points, a long-standing question mark, receives a surprising and simple answer below.

A microscopic model that exhibits first-order phase transitions within tricritical and critical end-point phase diagrams is the Blume-Emery-Griffiths model [6,7], with Hamiltonian

$$-\beta\mathcal{H} = \sum_{\langle ij\rangle} J s_i s_j + \sum_{\langle ij\rangle} K s_i^2 s_j^2 - \sum_i \Delta s_i^2 ,$$

where $s_i = 0, \pm 1$ at each site i of a lattice and $\langle ij\rangle$ indicates summation over all nearest-neighbor pairs of sites. This Hamiltonian can be rewritten as

$$\sum_{\langle ij\rangle} [J s_i s_j + K s_i^2 s_j^2 + D(s_i^2 + s_j^2) + D^{\dagger}(s_i^2 - s_j^2)] ,$$

where j is, on the cubic lattice, on the increasing coordinate side of i. The ordered phases of this model are up magnetized, $\langle s_i\rangle > 0$, and down magnetized, $\langle s_i\rangle < 0$. The symmetry that is broken is global spin-reversal symmetry. Since each of the terms in the Hamiltonian above is invariant under this symmetry, the corresponding coupling constants, $J, K, D, D^{\dagger}$, are bond strengths. Bond randomness obtains when the bond strengths vary randomly across the system, governed by a quenched probability distribution $P(J_{ij}, K_{ij}, D_{ij}, D_{ij}^{\dagger})$.

The renormalization-group solution of the quenched random system is via the recursion of the probability distribution [8–10], given by

$$P'(\mathbf{K}'_{i'j'}) = \int \left[\prod_{ij} d\mathbf{K}_{ij} P(\mathbf{K}_{ij}) \right] \delta(\mathbf{K}'_{i'j'} - \mathbf{R}(\{\mathbf{K}_{ij}\})) , \tag{1}$$

where $\mathbf{K}_{ij} \equiv (J_{ij}, K_{ij}, D_{ij}, D_{ij}^{\dagger})$, the primes refer to the rescaled system, $\mathbf{R}(\{\mathbf{K}_{ij}\})$ is a local recursion relation for the bond strengths, and the positional index ij runs through the localities of the unrenormalized system that effectively influence the renormalized interactions at the renormalized locality $i'j'$. A basic premise is that the crux of the quenched randomness problem lies in the convolution given in Eq. (1), i.e., that the novelties brought by the quenched randomness derive from the proper treatment of the functional integration in the equation, rather than the precise form of the local recursion relation. The integration complicates, after a few rescalings, even the simplest starting distribution. Thus, the level of approximation is defined by the level of detail of the form into which the renormalized distribution is forced.

The local recursion relation was obtained using the Migdal-Kadanoff procedure [11,12] in $d = 3$ dimensions with a length rescaling factor of $b = 2$. First, "bond moving" is performed, combining groups of b^{d-1} interactions:

$$\tilde{J}_{ij} = J_{i_1 j_1} + J_{i_2 j_2} + \cdots , \tag{2}$$

and similarly for the other coupling constants. Second, a decimation is performed, yielding the renormalized interactions:

$$J'_{i'j'} = \ln(R_3/R_4)/2 , \qquad D'_{i'j'} = \ln(R_1 R_2/R_0^2)/2 ,$$
$$K'_{i'j'} = \ln(R_0^2 R_3 R_4/R_1^2 R_2^2)/2 , \qquad D^{\dagger\prime}_{i'j'} = \ln(R_1/R_2)/2 , \tag{3}$$

where

 0031-9007/96/76(23)/4380(4)$10.00

$$
\begin{aligned}
R_0 &= 2\exp(\tilde{D}_{ij} - \tilde{D}^{\dagger}_{ij} + \tilde{D}_{jk} + \tilde{D}^{\dagger}_{jk}) + 1\,,\\
R_1 &= \exp(\tilde{J}_{ij} + \tilde{K}_{ij} + 2\tilde{D}_{ij} + \tilde{D}_{jk} + \tilde{D}^{\dagger}_{jk})\\
&\quad + \exp(-\tilde{J}_{ij} + \tilde{K}_{ij} + 2\tilde{D}_{ij} + \tilde{D}_{jk} + \tilde{D}^{\dagger}_{jk})\\
&\quad + \exp(\tilde{D}_{ij} + \tilde{D}^{\dagger}_{ij})\,,\\
R_2 &= \exp(\tilde{D}_{ij} - \tilde{D}^{\dagger}_{ij} + \tilde{J}_{jk} + \tilde{K}_{jk} + 2\tilde{D}_{jk})\\
&\quad + \exp(\tilde{D}_{ij} - \tilde{D}^{\dagger}_{ij} - \tilde{J}_{jk} + \tilde{K}_{jk} + 2\tilde{D}_{jk})\\
&\quad + \exp(\tilde{D}_{jk} - \tilde{D}^{\dagger}_{jk})\,,\\
R_3 &= \exp(\tilde{J}_{ij} + \tilde{K}_{ij} + 2\tilde{D}_{ij} + \tilde{J}_{jk} + \tilde{K}_{jk} + 2\tilde{D}_{jk})\\
&\quad + \exp(-\tilde{J}_{ij} + \tilde{K}_{ij} + 2\tilde{D}_{ij} - \tilde{J}_{jk} + \tilde{K}_{jk} + 2\tilde{D}_{jk})\\
&\quad + \exp(\tilde{D}_{ij} + \tilde{D}^{\dagger}_{ij} + \tilde{D}_{jk} - \tilde{D}^{\dagger}_{jk})\,,\\
R_4 &= \exp(\tilde{J}_{ij} + \tilde{K}_{ij} + 2\tilde{D}_{ij} - \tilde{J}_{jk} + \tilde{K}_{jk} + 2\tilde{D}_{jk})\\
&\quad + \exp(-\tilde{J}_{ij} + \tilde{K}_{ij} + 2\tilde{D}_{ij} + \tilde{J}_{jk} + \tilde{K}_{jk} + 2\tilde{D}_{jk})\\
&\quad + \exp(\tilde{D}_{ij} + \tilde{D}^{\dagger}_{ij} + \tilde{D}_{jk} - \tilde{D}^{\dagger}_{jk})\,.
\end{aligned}
$$

Equations (2) and (3) are approximate recursion relations for the cubic lattice and, simultaneously, exact recursion relations for a three-dimensional hierarchical lattice [13].

As mentioned above, the crux of our calculation consists in the evaluation of the probability convolution in Eq. (1), which we now detail. The initial quenched probability distribution has a symmetry, $P(J_{ij}, K_{ij}, D_{ij}, D^{\dagger}_{ij}) = P(J_{ij}, K_{ij}, D_{ij}, -D^{\dagger}_{ij})$, which is preserved under the renormalization-group transformation and which is calculationally exploited in the steps described below. The probability distribution $P(J_{ij}, K_{ij}, D_{ij}, D^{\dagger}_{ij})$ is represented by histograms. Each histogram is characterized by five quantities, $J_{ij}, K_{ij}, D_{ij}, D^{\dagger}_{ij}$ and the associated probability p. Our calculation consists of the following steps: (1) The histograms are placed on a grid in the space of interactions $J_{ij}, K_{ij}, D_{ij}, D^{\dagger}_{ij}$. All histograms that fall within the same grid cell are combined in such a way as to preserve the averages and standard deviations of the interactions. The histograms that fall outside the grid, representing a very small probability, are similarly combined into a single histogram. (2) Two distributions are convoluted as in Eq. (1) with $\mathbf{R}(\mathbf{K}_{i_1 j_1}\mathbf{K}_{i_2 j_2}) = \mathbf{K}_{i_1 j_1} + \mathbf{K}_{i_2 j_2}$, regenerating the original number of histograms. (3) The previous two steps are performed $d-1$ times, which completes the implementation of bond moving, Eq. (2), for quenched random interactions. (4) The two steps are again repeated, but this time with $\mathbf{R}$ as given by the decimation of Eq. (3). This completes the entire renormalization-group transformation, yielding the histograms for the renormalized quenched probability distribution $P'(J'_{i'j'}, K'_{i'j'}, D'_{i'j'}, D^{\dagger\prime}_{i'j'})$. Most of our calculations have used up to 13 530 independent ($D^{\dagger}_{ij} \geq 0$) histograms, with corresponding renormalization-group flows of 67 650 quantities. Several more detailed calculations, involving the renormalization-group flows of 3 921 890 quantities, confirmed the numerical accuracy of our procedure.

The thermodynamic densities are obtained within the renormalization-group calculation [9]. Using the chain rule,

$$
\mathbf{n} = \frac{1}{N}\sum_{\langle ij\rangle}\frac{\partial \ln Z}{\partial \mathbf{K}_{ij}} = \frac{1}{N}\sum_{\langle i'j'\rangle}\frac{\partial \ln Z}{\partial \mathbf{K}'_{i'j'}}\cdot\sum_{\langle ij\rangle}^{\langle i'j'\rangle}\frac{\partial \mathbf{K}'_{i'j'}}{\partial \mathbf{K}_{ij}}\,,
$$

where N is the number of nearest-neighbor pairs and Z is the partition function. The last sum is over the b^d unrenormalized pairs $\langle ij\rangle$ contributing to the renormalized pair $\langle i'j'\rangle$. This sum is replaced, as an approximation, by its average value,

$$
\sum_{\langle ij\rangle}^{\langle i'j'\rangle}\frac{\partial \mathbf{K}'_{i'j'}}{\partial \mathbf{K}_{ij}} \cong \int\left[\prod_{\langle ij\rangle}^{\langle i'j'\rangle} d\mathbf{K}_{ij}P(\mathbf{K}_{ij})\right]\sum_{\langle ij\rangle}^{\langle i'j'\rangle}\frac{\partial \mathbf{K}'_{i'j'}}{\partial \mathbf{K}_{ij}} \equiv \frac{\partial \mathbf{K}'}{\partial \mathbf{K}}\,,
$$

which yields the simple density recursion relation $\mathbf{n} \cong b^{-d}\mathbf{n}'\cdot\partial\mathbf{K}'/\partial\mathbf{K}$. Repeated applications of this recursion relation connect the thermodynamic densities of a trajectory initial point and phase-sink fixed point, permitting the evaluation of the former.

We find that, in $d = 2$, in quenched random-bond systems with the initial distribution

$$
\begin{aligned}
P(\mathbf{K}_{ij}) = {}& \delta(K_{ij} - K)\delta(D_{ij} - D)\delta(D^{\dagger}_{ij})\\
&\times[\delta(J_{ij} - J - \sigma) + \delta(J_{ij} - J + \sigma)]/2\,, \quad (4)
\end{aligned}
$$

all symmetry-breaking first-order phase transitions are converted to second-order, and all non-symmetry-breaking first-order phase transitions are eliminated [1,2,5]. These results are illustrated with $\sigma = J/4$ in Fig. 1, for systems that have tricritical (e.g., for $K/J = 0$) and critical end-point (e.g., for $K/J = 4$) phase diagrams before the introduction of bond randomness. We have also verified that the phase boundaries for both cases are converted to second order down to zero temperature with randomness as small as $\sigma = J/100$. Under the increased accuracy of our present calculations, the reentrance seen in preliminary (done with only 8 independent histograms, as opposed to 13 530 or more here) calculations [5] is eliminated.

We find qualitatively different behavior in $d = 3$. We first discuss our results for $K/J = 0$ [Figs. 2(a)–2(c)], for which the pure (nonrandom) system has a tricritical phase diagram. Upon introduction of quenched bond randomness, the pure-system tricritical point is replaced by a line segment of second-order phase transitions dominated by randomness, that is renormalizing to a fixed distribution with nonzero widths. This line segment is bounded by a multicritical point and a random-bond tricritical point, which are separately dominated by randomness. The fixed distributions are characterized in Table I in terms of their averages and standard deviations, $\overline{J} = \int d\mathbf{K}_{ij}P(\mathbf{K}_{ij})J_{ij}$ and

$$
\sigma_J = \left[\int d\mathbf{K}_{ij}\,P(\mathbf{K}_{ij})\,(J_{ij} - \overline{J})^2\right]^{1/2}, \quad (5)
$$

and similarly for the other coupling constants. Thus, at

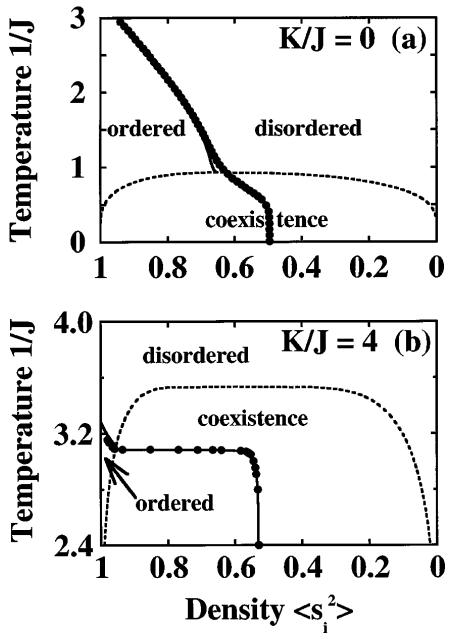

FIG. 1. In $d = 2$, the effect of bond randomness on (a) tricritical and (b) critical end-point phase diagrams. The unrenormalized system has the quenched random-bond distribution of Eq. (4) with $\sigma = J/4$. The solid circles represent the phase boundary points, which are all second order, of the random-bond system. For reference, the phase diagrams of the nonrandom systems are drawn with the undotted lines, showing coexistence boundaries (dashed) of first-order phase transitions.

one end of the new segment, the multicritical point separates two different lines of second-order phase transitions, each with its own fixed point of fixed distribution reached under repeated rescalings. Accordingly, the phase transition points of each line have the same critical exponents, which differ between the two lines, in violation of the empirical universality principle [14]. At the other end of the new segment, the random-bond tricritical point separates this second-order line segment and the coexistence region of a first-order phase transition. As seen in Figs. 2(a) and 2(b), the coexistence boundaries drop very sharply to the tricritical point. Although this behavior appears discontinuous in the figures, in reality it corresponds to an extremely small, but still positive tricritical exponent $\beta_u = 0.020$. This is ascertained because we find that the fixed distribution of the random-bond tricritical point (Fig. 3) is, in fact, the fixed distribution of the random-field Ising criticality [10], with the identifications

$$I_{ij} = (J_{ij} + K_{ij})/4, \qquad H_{ij} = (J_{ij} + K_{ij})/2 + D_{ij},$$
$$H_{ij}^{\dagger} = D_{ij}^{\dagger}, \qquad G_{ij} = (J_{ij} + K_{ij})/4 + D_{ij}, \tag{6}$$

valid at $J_{ij} \to \infty$, referring to the random-field Ising Hamiltonian

$$\sum_{\langle ij \rangle} [I_{ij} s_i s_j + H_{ij}(s_i + s_j)/2 + H_{ij}^{\dagger}(s_i - s_j)/2 + G_{ij}],$$

where $s_i = \pm 1$ at each site i.

Phase diagrams qualitatively similar to Figs. 2(a) and 2(b) are obtained with quenched randomness in J [e.g., Eq. (4)] that does not include negative, viz. antiferromagnetic, values. With this restriction, randomness in J cannot be made strong enough to eliminate all first-order transitions. However, quenched bond randomness, without the calculational complication of frustration, can be studied with the initial distribution

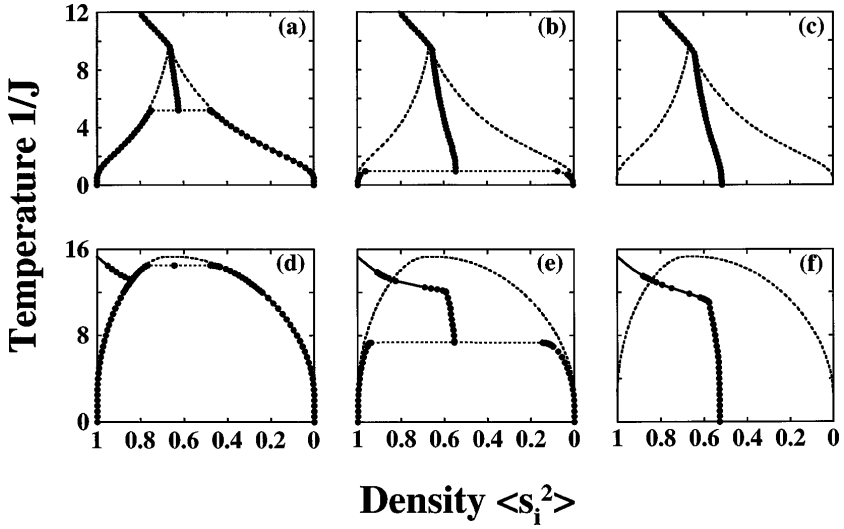

FIG. 2. In $d = 3$, the effect of bond randomness on (a)–(c) tricritical, $K/J = 0$, and (d)–(f) critical end-point, $K/J = 4$, phase diagrams. The unrenormalized system has the quenched random-bond distribution of Eq. (7) with (a) $\sigma/J = 0.2$, (b) $\sigma/J = 0.527$, (c) $\sigma/J = 1$, (d) $\sigma/J = 0.13$, (e) $\sigma/J = 2$, (f) $\sigma/J = 4$. The solid circles represent the phase boundary points, which include second-order transitions and coexistence boundaries [which recede as randomness is increased from (a) to (c) or from (d) to (f)], of the random-bond system. In (a)–(c) and (e) and (f), the joining, at a multicritical point, of two second-order lines (having different critical properties), in the absence of any other phase-transition line going through the multicritical point, constitutes the violation of the empirical universality principle. For reference, the phase diagrams of the nonrandom systems are drawn with the undotted lines, showing coexistence boundaries (dashed) of first-order phase transitions.

TABLE I. Averages and standard deviations [see Eq. (5)] at fixed distributions for the new second-order segment (N^*), the multicritical point (M^*), and the random-bond tricritical point (R^*)

	$\overline{J}, \overline{K}, \overline{D}, \overline{D}^\dagger$	$\sigma_J, \sigma_K, \sigma_D, \sigma_{D\dagger}$
N^*	$\infty, -0.355 - \overline{J}, 0.176, 0$	$1.250\overline{J}, -1.250\overline{K}, \infty, \infty$
M^*	$0.183, -0.028, 0.026, 0$	$0.155, 0.041, \infty, \infty$
R^*	$\infty, 0.418\overline{J}, 0.709\overline{J}, 0$	$0.297\overline{J}, 1.211\overline{K}, 1.011\overline{D}, 0.512\overline{D}$

$$P(\mathbf{K}_{ij}) = \delta(J_{ij} - J)\delta(K_{ij} - K)[\delta(D_{ij} - D - \sigma) \times \delta(D_{ij}^\dagger) + \delta(D_{ij} - D + \sigma)\delta(D_{ij}^\dagger) + \delta(D_{ij} - D) \times \delta(D_{ij}^\dagger - \sigma) + \delta(D_{ij} - D)\delta(D_{ij}^\dagger + \sigma)]/4. \quad (7)$$

Recall that the symmetry that is broken is global spin-reversal symmetry and, since each of the terms in the Hamiltonian is invariant under this symmetry, each of the corresponding coupling constants, J, K, D, or $D^\dagger$, is a bond strength. Thus, Fig. 2(c) shows that, with sufficient amount of quenched bond randomness, the first-order phase transition is entirely eliminated via the random-bond tricritical point reaching zero temperature.

Figures 2(d)–2(f) show our results for $K/J = 4$, for which the pure system has a critical end-point phase diagram. Forsmall amounts of bond randomness, the critical end-point phase diagram persists, with the isolated critical point lowered in temperature and transformed to a random-field Ising critical point [Fig. 2(d)]. This can be seen from the very precipitous behavior of the coexistence boundary, correspond to a very small but positive critical exponents $\beta = 0.020$ [10,15], equal to the tricritical β_u above. As bond randomness is increased, the random-bond tricritical phase diagram [Fig. 2(e)] and the fully second-order phase diagram [Fig. 2(f)] are obtained. These phase diagrams have been discussed above.

An experimental verification of this violation of universality is of course called for. A prime candidate for this study is the onset of superfluidity in helium mixtures immersed in aerogel [16,17].

This research was supported by the U.S. Department of Energy under Grant No. DE-FG02-92ER45473.

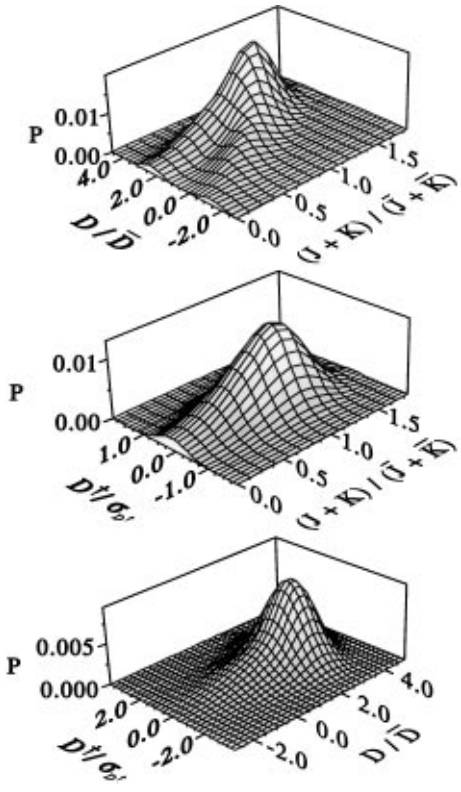

FIG. 3. In $d = 3$, the random-bond tricritical fixed distribution. With the associations of Eq. (6), this fixed distribution is equivalent to the fixed distribution of random-field Ising criticality [10].

[1] A. N. Berker, J. Appl. Phys. **70**, 5941 (1991).
[2] A. N. Berker, Physica (Amsterdam) **194A**, 72 (1993).
[3] A. N. Berker and A. Falicov, Tr. J. Phys. **18**, 347 (1994).
[4] J. Wehr and M. Aizenman, Phys. Rev. Lett. **62**, 2503 (1989).
[5] K. Hui and A. N. Berker, Phys. Rev. Lett. **62**, 2507 (1989); **63**, 2433(E) (1989).
[6] M. Blume, V. J. Emery, and R. B. Griffiths, Phys. Rev. A **4**, 1071 (1971).
[7] For experimental applications see [6] for helium mixtures; J. Lajzerowicz and J. Sivardière, Phys. Rev. A **11**, 2079 (1975); J. Sivardière and J. Lajzerowicz, *ibid.* **11**, 2090 (1975); **11**, 2101 (1975), for solid-liquid-gas systems, multicomponent fluid and liquid crystal mixtures; M. Schick and W.-H. Shih, Phys. Rev. B **34**, 1797 (1986), for microemulsions; and K. E. Newman and J. D. Dow, Phys. Rev. B **27**, 7495 (1983), for semiconductor alloys.
[8] D. Andelman and A. N. Berker, Phys. Rev. B **29**, 2630 (1984).
[9] S. R. McKay and A. N. Berker, J. Appl. Phys. **64**, 5785 (1988).
[10] A. Falicov, A. N. Berker, and S. R. McKay, Phys. Rev. B **51**, 8266 (1995).
[11] A. A. Migdal, Zh. Eksp. Teor. Fiz **69**, 1457 (1975) [Sov. Phys. JETP **42**, 743 (1976)].
[12] L. P. Kadanoff, Ann. Phys. (N.Y.) **100**, 359 (1976).
[13] A. N. Berker and S. Ostlund, J. Phys. C **12**, 4961 (1979).
[14] This universality violation was also seen independently in M. Kardar, A. L. Stella, G. Sartoni, and B. Derrida, Phys. Rev. E **52**, R1269 (1995). In this work, it was discovered that random-bond q-state Potts models have q-independent critical behavior dominated by strong randomness, distinct from their q-dependent critical behavior dominated by weak randomness found in [8].
[15] M. S. Cao and J. Machta, Phys. Rev. B **48**, 3177 (1993).
[16] S. B. Kim, J. Ma, and M. H. W. Chan, Phys. Rev. Lett. **71**, 2268 (1993).
[17] A. Falicov and A. N. Berker, Phys. Rev. Lett. **74**, 426 (1995). In this paper, a phase diagram, qualitatively different from the ones here, is induced by *correlated* bond randomness.